

The phase diagram and the structure of CDW state in high magnetic field in quasi-1D materials: mean-field approach

P. D. Grigoriev

National High Magnetic Field laboratory, Florida State University, Tallahassee, Florida *

D. S. Lyubshin

L. D. Landau Institute for Theoretical Physics, 142432 Chernogolovka, Russia

(Dated: December 18, 2018)

We develop the mean-field theory of a charge-density wave (CDW) state in magnetic field and study the properties of this state below the transition temperature. We show that the CDW state with shifted wave vector in high magnetic field (CDW_x phase) has at least double harmonic modulation on the most part of the phase diagram. In the perfect nesting case the single harmonic CDW state with shifted wave vector exists only in a very narrow region near the tricritical point where the fluctuations are very strong. We show that the transition from CDW₀ to CDW_x state below the critical temperature is accompanied by a jump of the CDW order parameter and of the wave vector rather than by their continuous increase. This implies a first order transition between these CDW states and explains the strong hysteresis accompanying this transition in many experiments. We examine how the phase diagram changes in the case of imperfect nesting.

PACS numbers: 71.30.+h, 71.45.Lr, 74.70.Kn

I. INTRODUCTION

The properties of metals with a charge-density-wave (CDW) ground state attract great attention since the fifties (see, e.g., monographs [1,2]). In quasi-1D metals, the Fermi surface (FS) consists of two slightly warped sheets separated by $2k_F$ and roughly possesses the nesting property that leads to the Peierls instability and favors the formation of the charge- or spin-density-wave (SDW) state at low temperature.

The mean-field description is known to be unable to describe strictly 1D conductors, where the non-perturbative methods and exactly solvable models are of great importance.³ However, in most materials manifesting CDW or SDW phenomena the nonzero value of the electron transfer integral between conducting chains and the 3D character of the electron-electron interactions and lattice elasticity reduce the deviations from the mean-field solution and also make most of the methods and exactly solvable models developed for strictly 1D case inapplicable.⁴ The effect of fluctuations in Q1D metals and their influence on the mean-field description of the Peierls transition in these metals has been considered in a number of papers (see e.g. [5,6] and references therein). It was shown that the interchain dispersion of electrons strongly damps the fluctuation and validate the mean-field description. In Q1D organic metals,⁷ at which our present study is mainly aimed, the free electron dispersion near the Fermi level is, approximately, given by

$$\varepsilon_\sigma(\mathbf{k}) = \hbar v_F(|k_x| - k_F) - t_\perp(\mathbf{k}_\perp) - \sigma H, \quad (1)$$

where v_F and k_F are the Fermi velocity and Fermi momentum in the chain (x) direction, $H \equiv \mu_B B$ is the Zeeman energy, μ_B is the Bohr magneton and B is the external magnetic field. The perpendicular-to-chain term, $t_\perp(\mathbf{k}_\perp)$, is much greater than the energy scale of the

CDW(SDW) transition temperature, T_{c0} . Only the "imperfect nesting" part, t'_b , of $t_\perp(\mathbf{k}_\perp)$ is of the order of T_{c0} (see Eqs. (2), (3)). Hence, the criterion for the mean-field theory to be applicable,^{5,6} $t_\perp \gg T_{c0}$, is reliably satisfied in most Q1D organic metals.

The mean-field description of the CDW properties is, in many aspects, very similar to the BCS theory. The pairing of two electrons in superconductors is replaced in CDW by the pairing of an electron with the hole on the opposite sheet of the Fermi surface. The charge and spin coupling constants in CDW (see interaction Hamiltonian (5)) are analogous to coupling constants in spin-singlet and spin-triplet channels in superconductivity. The CDW phase with shifted nesting vector is similar to the non-uniform superconducting phase (LOFF phase).^{8,9} However, there are several important differences between these two many-particle effects. The first difference is that the formation of a gap in the electron spectrum in CDW leads to an insulating rather than superconducting state. This happens due to the pinning of the CDW condensate by crystal imperfections. Hence, the CDW state does not reveal a superfluid current.^{1,2} Other differences appear, e.g., in the excitation spectrum. In particular, the lowest energy excitations in magnetic field or at imperfect nesting are not always the electron pairs as in BCS theory but may be the "soliton kinks".¹⁰⁻¹⁴

The theoretical investigation of the CDW/SDW properties at a mean-field level comprises two main branches. The first focuses on the transition line from the metallic states to CDW/SDW state using susceptibility calculations. This allows to include many additional factors into the theoretical model, such as different free electron dispersion relations, spin and orbital effects of the external magnetic field, applied pressure etc. It helped to discover and to explain many beautiful effects such as the field-induced spin- and charge-density waves (FISDW),¹⁸⁻²¹

the increase of the transition temperature due to the one-dimensionization of the electron spectrum in high magnetic field,^{18,23} the CDW state with shifted nesting vector^{19,24}) etc. However, all these results cannot be continued below the transition temperature since they are based on the electron susceptibility calculations using metallic-state electron Green's functions. In particular, the calculation of [24] predicts an appearance of the CDW_x phase with shifted wave vector as the magnetic field exceeds some critical value. This calculation gives the metal- CDW_x transition line, $T_c(H)$, and the dependence of the optimal shift $q_x(H)$ of CDW wave vector on magnetic field at this transition line. However, this calculation does not extend below the transition temperature, and, hence, cannot be used to describe the properties and the phase diagram inside the CDW phase. For example, it neither describes the structure of the CDW_x phase below $T_c(H)$ nor gives the CDW_0 - CDW_x transition line $H_{c1}(T)$ or the kind of this transition. The mean-field study of CDW in Ref. [22] is applicable only in weak field when the CDW wave vector does not shift from its zero-field value.

The second branch of investigation involves the soliton physics. It appeared first to describe the ground state of polyacetylene^{10,11} and then developed into a rather large activity (see Refs. [15,16] for a review). In particular, the soliton structure and the energy spectrum of CDW state in external magnetic field were considered¹⁷. However, all these results were only derived at zero temperature and perfect nesting and are not applicable at temperatures of the order of transition temperature, $T \sim T_c$. The finite-temperature phase transition to soliton phase has been considered in Ref. [14]. However, that phase diagram refers to zero field and finite shift of the chemical potential from the value μ_0 corresponding to the commensurate CDW.¹⁴ The analysis of the CDW phase diagram in magnetic field has been performed in the case of perfect nesting and at the electron density close to half-filling.²⁵ However, this approach is also unable to describe the incommensurate case far from half-filling. In particular, it suggests the one-harmonic modulation of charge density, which is usually unstable in high magnetic field (see below).

Further theoretical description of the CDW state in magnetic field became important last years because of the intensive experimental study of the CDW state in strongly anisotropic organic metals.²⁶⁻³⁶

In the present paper we study the CDW phase diagram and the properties of the CDW state at finite temperature below the transition point in the mean-field approximation. This study links the results of susceptibility calculations and the results from the soliton approach. We take into account the spin effect of the external magnetic field and consider the CDW phase with shifted nesting vector. The "antnesting" term in the electron dispersion is also taken into account. We show that the CDW_x state with shifted wave vector, proposed in Ref. [24], has double harmonic modulation almost everywhere in the phase diagram (see Fig. 3,5). At perfect nesting, $t'_b = 0$, the

single harmonic CDW_x state exists only in a very narrow region near the tricritical point. We show that the transition from CDW_0 to CDW_x state below the critical temperature is accompanied by a jump of the CDW wave vector rather than by its continuous increase. This implies a first order transition between the CDW states and explains the strong hysteresis observed at the kink transition.^{28,29,32,34}

Besides the Zeeman splitting, external magnetic field affects the orbital electron motion. First, an external magnetic field perpendicular to conducting layers leads to one-dimensionization of the electron spectrum in quasi-1D metals²³ that improves the nesting property of the Fermi surface. Second, due to the strong scattering by the nesting vector, electrons in quasi-1D metal in magnetic field may form close orbits in momentum space¹⁹. These orbital effects increase the CDW or SDW transition temperature and may lead to the field-induced spin-density waves¹⁸ (for a review, see [7]). A similar effect for the charge density waves was also proposed²¹. The interplay between spin and orbital effects of the magnetic field is quite interesting. It leads, for example, to a series of phase transitions between the CDW states with quantized nesting vector.³²

In our present study we disregard the orbital effects of magnetic field. This limitation, however, is not very restrictive. If the magnetic field is parallel to the conducting layers, it produces only the Zeeman splitting and no orbital effect. The orbital quantization effects are, usually, more subtle than the spin effect. As an illustration, the quantized nesting phases can be observed only at very low temperature³² because the effects of nesting quantization are strongly damped at $\hbar\omega_c = e\hbar H/m^*c \ll 2\pi T, 2\pi\hbar/\tau, \Delta$. This damping is somewhat similar to that of the magnetic quantum oscillations. The one-dimensionalization of electron spectrum in magnetic field can be effectively taken into account in the present study by introducing the magnetic field dependence of the imperfect nesting transfer integral, $t'(H)$, in the electron dispersion relation (2). A situation which is mathematically equivalent to the Zeeman splitting of magnetic field without its orbital effect arises when there are two slightly different Q1D chain system in the same compound with coupling between the chains of different type. The quantities $U_c + U_s$ and $U_c - U_s$ play the role of the electron coupling constant inside the chains and between the chains of different type, respectively. Such a system occurs in many compounds as TTF-type organic metals (see, e.g., the discussion on page 196 in [16]). Two slightly different types of chains occur also in $\alpha\text{-}(\text{Per})_2\text{M}(\text{mnt})_2$.³⁵⁻³⁷ In the systems with molecular chains of two types, however, the difference between optimal CDW wave vectors on different chains is fixed by the molecular structure and does not vary as in the case of external magnetic field which gradually separates the Fermi surfaces with two different spin components.

II. THE MODEL AND THE MEAN-FIELD THEORY OF CDW IN MAGNETIC FIELD.

1.. The model

We consider a quasi-1D metal with dispersion (1) and $t_{\perp}(\mathbf{k}_{\perp})$ given by the tight-binding model:

$$t_{\perp}(\mathbf{k}_{\perp}) = -2t_b \cos(k_y b) - 2t'_b \cos(2k_y b) - 2t_c \cos(k_z c_z), \quad (2)$$

where b and c_z are the lattice constants in y - and z -directions respectively. The dispersion along the z -axis is assumed to be much weaker than the dispersion along y -direction. Therefore, we omit the second harmonic $\propto \cos(2k_z c_z)$ in the dispersion relation (2). Since the terms $2t_c \cos(k_z c_z)$ and $2t_b \cos(k_y b)$ do not violate the perfect nesting condition

$$\varepsilon(\mathbf{p} + \mathbf{Q}) = -\varepsilon(\mathbf{p}), \quad (3)$$

they do not influence the physics discussed below unless the nesting vector become shifted in y - z plane. We do not consider such a shift in the present study.

The electron Hamiltonian is

$$\hat{H} = \hat{H}_0 + \hat{H}_{\text{int}},$$

with the free-electron part

$$\hat{H}_0 = \sum_{\mathbf{k}\sigma} \varepsilon_{\sigma}(\mathbf{k}) a_{\sigma}^{\dagger}(\mathbf{k}) a_{\sigma}(\mathbf{k}) \quad (4)$$

and the interaction part

$$\begin{aligned} \hat{H}_{\text{int}} = \frac{1}{2} \sum_{\mathbf{k}\mathbf{k}'\mathbf{Q}\sigma\sigma'} V_{\sigma\sigma'}(\mathbf{Q}) a_{\sigma}^{\dagger}(\mathbf{k} + \mathbf{Q}) a_{\sigma}(\mathbf{k}) \\ \times a_{\sigma'}^{\dagger}(\mathbf{k}' - \mathbf{Q}) a_{\sigma'}(\mathbf{k}'). \end{aligned} \quad (5)$$

This Hamiltonian does not include the orbital effect of magnetic field on quasi-1D electron spectrum which may be important in the case of substantially imperfect nesting and strong magnetic field perpendicular to the easy-conducting plane (see introduction). Later on we will be interested mainly in the interaction at the wave vector \mathbf{Q} close to the so-called nesting vector \mathbf{Q}_0 , which is usually chosen as

$$\mathbf{Q}_0 = (\pm 2k_F, \pi/b, \pi/c). \quad (6)$$

The deviations $\mathbf{Q} - \mathbf{Q}_0$ that will be considered below are of the order of $\max\{H, t'_b\}/\hbar v_F \ll k_F$, so that for such small deviations the interaction function

$$V_{\sigma\sigma'}(\mathbf{Q}) \approx V_{\sigma\sigma'}(\mathbf{Q} = \mathbf{Q}_0) = U_c - U_s \sigma \sigma' \quad (7)$$

The coupling constants U_c and U_s are the same as in Ref. [24]. Subscripts c and s distinguish charge and spin coupling constants. The Hamiltonian (5) can be obtained from the extended Hubbard model when the e-e scattering by the momenta close to the nesting wave vector \mathbf{Q}_0 is only taken in to account.

2.. Mean field approach

First, we note that the terms with $\mathbf{Q} = 0$ in (5) only renormalizes the chemical potential and will not be omitted in subsequent calculations (all sums over \mathbf{Q} do not include $\mathbf{Q} = 0$). We introduce the thermodynamic Green's function

$$g_{\sigma}(\mathbf{k}', \mathbf{k}, \tau - \tau') = \langle T_{\tau} \{ a_{\sigma}^{\dagger}(\mathbf{k}', \tau') a_{\sigma}(\mathbf{k}, \tau) \} \rangle, \quad (8)$$

where the operators are taken in the Heisenberg representation, and the average

$$D_{\mathbf{Q}\sigma} = \sum_{\mathbf{k}} g_{\sigma}(\mathbf{k} - \mathbf{Q}, \mathbf{k}, -0) - \delta(\mathbf{Q}, 0) n_{\sigma}. \quad (9)$$

After defining

$$\Delta_{\mathbf{Q}\sigma} = \sum_{\sigma'} (U_c - U_s \sigma \sigma') D_{\mathbf{Q}\sigma'} \quad (10)$$

one obtains in the mean-field approximation

$$\hat{H}_{\text{int}} = \sum_{\mathbf{Q}\mathbf{k}\sigma} a_{\sigma}^{\dagger}(\mathbf{k} + \mathbf{Q}) a_{\sigma}(\mathbf{k}) \Delta_{\mathbf{Q}\sigma} - \frac{1}{2} \sum_{\mathbf{Q}\sigma} D_{-\mathbf{Q}\sigma} \Delta_{\mathbf{Q}\sigma}. \quad (11)$$

Hermiticity of the Hamiltonian requires $\Delta_{-\mathbf{Q}\sigma} = \Delta_{\mathbf{Q}\sigma}^*$. It is now straightforward to write down the equations of motion which in the frequency representation take the form

$$\begin{aligned} [i\omega - \varepsilon_{\sigma}(\mathbf{k})] g_{\sigma}(\mathbf{k}', \mathbf{k}, \omega) - \sum_{\mathbf{Q}} \Delta_{\mathbf{Q}\sigma} g_{\sigma}(\mathbf{k}', \mathbf{k} - \mathbf{Q}, \omega) \\ = \delta(\mathbf{k}', \mathbf{k}). \end{aligned} \quad (12)$$

3.. The Cosine Phase

Now we consider the solution with $\Delta_{\mathbf{k}\sigma} \neq 0$ only for $\mathbf{k} = \pm \mathbf{Q}$, where $\mathbf{Q} = 2k_F \mathbf{e}_x + (\pi/b) \mathbf{e}_y + \mathbf{q}$ with $|\mathbf{q}| \ll k_F$. If we neglect the scattering into the states with $|k_x| \gtrsim 2k_F$, the equations (12) decouple: for $k_x > 0$ one has

$$\begin{pmatrix} i\omega - \varepsilon_{\sigma}(\mathbf{k}) & -\Delta_{\mathbf{Q}\sigma} \\ -\Delta_{-\mathbf{Q}\sigma} & i\omega - \varepsilon_{\sigma}(\mathbf{k} - \mathbf{Q}) \end{pmatrix} \hat{G} = \hat{I}, \quad (13)$$

where

$$\hat{G} \equiv \begin{pmatrix} g_{\sigma}(\mathbf{k}, \mathbf{k}, \omega) & g_{\sigma}(\mathbf{k} - \mathbf{Q}, \mathbf{k}, \omega) \\ g_{\sigma}(\mathbf{k}, \mathbf{k} - \mathbf{Q}, \omega) & g_{\sigma}(\mathbf{k} - \mathbf{Q}, \mathbf{k} - \mathbf{Q}, \omega) \end{pmatrix} \quad (14)$$

and \hat{I} is the 2×2 identity matrix. The equation for $k_x < 0$ may be obtained via a substitution $\mathbf{Q} \rightarrow -\mathbf{Q}$. Introducing the notations

$$\varepsilon_{\sigma}^{\pm}(\mathbf{k}', \mathbf{k}) = \frac{\varepsilon_{\sigma}(\mathbf{k}') \pm \varepsilon_{\sigma}(\mathbf{k})}{2} \quad (15)$$

and using $\Delta_{\mathbf{Q}\sigma} \Delta_{-\mathbf{Q}\sigma} = |\Delta_{\mathbf{Q}\sigma}|^2$ from (13) one has

$$\begin{aligned}
g_\sigma(\mathbf{k} - \mathbf{Q}, \mathbf{k}, \omega) &= -\frac{\Delta_{\mathbf{Q}\sigma}}{[\omega + i\varepsilon_\sigma(\mathbf{k})][\omega + i\varepsilon_\sigma(\mathbf{k} - \mathbf{Q})] + |\Delta_{\mathbf{Q}\sigma}|^2} \\
&= -\frac{\Delta_{\mathbf{Q}\sigma}}{[\omega + i\varepsilon_\sigma^+(\mathbf{k}, \mathbf{k} - \mathbf{Q})]^2 + [\varepsilon_\sigma^-(\mathbf{k}, \mathbf{k} - \mathbf{Q})]^2 + |\Delta_{\mathbf{Q}\sigma}|^2}.
\end{aligned} \tag{16}$$

The consistency equation therefore is

$$\Delta_{\mathbf{Q}\sigma'} = -T \sum_{\mathbf{k}\omega\sigma} \frac{(U_c - U_s\sigma\sigma')\Delta_{\mathbf{Q}\sigma}}{[\omega + i\varepsilon_\sigma^+(\mathbf{k}, \mathbf{k} - \mathbf{Q})]^2 + [\varepsilon_\sigma^-(\mathbf{k}, \mathbf{k} - \mathbf{Q})]^2 + |\Delta_{\mathbf{Q}\sigma}|^2}. \tag{17}$$

where ω takes the values $\pi T(2n + 1)$, $n \in \mathbb{Z}$. Using the identity

$$T \sum_{\omega} \frac{1}{(\omega - i\alpha)^2 + a^2} = \frac{1}{4a} \left\{ \operatorname{th} \frac{a - \alpha}{2T} + \operatorname{th} \frac{a + \alpha}{2T} \right\}$$

this may be rewritten as

$$\Delta_{\mathbf{Q}\sigma'} = -\frac{1}{4} \sum_{\mathbf{k}\sigma} \frac{(U_c - U_s\sigma\sigma')\Delta_{\mathbf{Q}\sigma}}{\sqrt{|\Delta_{\mathbf{Q}\sigma}|^2 + [\varepsilon_\sigma^-(\mathbf{k}, \mathbf{k} - \mathbf{Q})]^2}} \left\{ \operatorname{th} \frac{E_{\sigma,+}(\mathbf{k})}{2T} - \operatorname{th} \frac{E_{\sigma,-}(\mathbf{k})}{2T} \right\}, \tag{18}$$

where

$$E_{\sigma,\pm}(\mathbf{k}) = \varepsilon_\sigma^+(\mathbf{k}, \mathbf{k} - \mathbf{Q}) \pm \sqrt{|\Delta_{\mathbf{Q}\sigma}|^2 + [\varepsilon_\sigma^-(\mathbf{k}, \mathbf{k} - \mathbf{Q})]^2} \tag{19}$$

is the energy spectrum in the cosine phase. From (2) it follows that for the right-moving electrons

$$\varepsilon_\sigma^+(\mathbf{k}, \mathbf{k} - \mathbf{Q}) = \frac{\hbar v_F q_x}{2} + 2t_b \sin \frac{q_y b}{2} \sin \left(k_y b - \frac{q_y b}{2} \right) - 2t'_b \cos q_y b \cos(2k_y b - q_y b) - \sigma H, \tag{20}$$

$$\varepsilon_\sigma^-(\mathbf{k}, \mathbf{k} - \mathbf{Q}) = \hbar v_F (k_x - k_F - q_x/2) - 2t_b \cos \frac{q_y b}{2} \cos \left(k_y b - \frac{q_y b}{2} \right) + 2t'_b \sin q_y b \sin(2k_y b - q_y b). \tag{21}$$

It is, however, more convenient to perform the momentum summation in Eq. (17) first. Extending the limits of the summation over k_x to infinity, one has

$$\Delta_{\mathbf{Q}\sigma'} = \frac{\pi\nu_F|U_c|T}{2} \sum_{\omega\sigma} \left\langle \frac{(1 + \nu\sigma\sigma')\Delta_{\mathbf{Q}\sigma}}{\sqrt{[\omega + i\varepsilon_\sigma^+(\mathbf{k}, \mathbf{k} - \mathbf{Q})]^2 + |\Delta_{\mathbf{Q}\sigma}|^2}} \right\rangle_{k_y}, \tag{22}$$

where the branch of the square root with positive real part is implied, the angular brackets stand for the averaging over all values of k_y , and we introduced the standard notation

$$\nu = -U_s/U_c \tag{23}$$

for the coupling ratio and

$$\nu_F = \frac{L_x}{\pi\hbar v_F} \tag{24}$$

for the density of states on the Fermi level per one spin component.

Expansion to the third order in $\Delta_{\mathbf{Q}\sigma}$ yields

$$\Delta_{\mathbf{Q}\sigma'} = \sum_{\sigma} \frac{1 + \nu\sigma\sigma'}{2} \left(K_\sigma^{(1)} - |\Delta_{\mathbf{Q}\sigma}|^2 K_\sigma^{(3)c} \right) \Delta_{\mathbf{Q}\sigma} \tag{25}$$

(the superscript “c” stands for “cosine”) with

$$K_\sigma^{(1)} = \pi\nu_F|U_c|T \sum_{\omega} \left\langle \frac{\operatorname{sign} \omega}{\omega + i\varepsilon_\sigma^+(\mathbf{k}, \mathbf{k} - \mathbf{Q})} \right\rangle_{k_y}, \tag{26}$$

$$K_\sigma^{(3)c} = \frac{\pi\nu_F|U_c|T}{2} \sum_{\omega} \left\langle \frac{\operatorname{sign} \omega}{(\omega + i\varepsilon_\sigma^+(\mathbf{k}, \mathbf{k} - \mathbf{Q}))^3} \right\rangle_{k_y}. \tag{27}$$

The second-order transition line corresponds to

$$\det \begin{pmatrix} \frac{1+\nu}{2} K_+^{(1)} - 1 & \frac{1-\nu}{2} K_-^{(1)} \\ \frac{1-\nu}{2} K_+^{(1)} & \frac{1+\nu}{2} K_-^{(1)} - 1 \end{pmatrix} = 0. \tag{28}$$

The left hand side of this equation is a function of ν, T, H and \mathbf{q} . The normal to CDW phase transition occurs at

some optimal value of \mathbf{q} which corresponds to the minimum of the free energy of the CDW state, that at the transition point is equivalent to the maximum of T_c or to the minimum of l.h.s. of Eq. (28).

Unrestricted summation over k_x introduced divergence into the summation over ω in $K_\sigma^{(1)}$, which may be renormalized by introducing the zero-field and zero- t'_b transition temperature T_{c0} . To obtain a closed expression for the latter, we note that for $H = 0$ one has $K_+^{(1)} = K_-^{(1)}$, and the matrix in (28) has eigenvalues $K_\sigma^{(1)} - 1$ and

$\nu K_\sigma^{(1)} - 1$. Therefore, at $H = 0$ $K_\sigma^{(1)}(T = T_c(t'_b), H = 0) = 1$. From (26) at $t'_b = 0$ after imposing a cutoff at $\omega \sim E_F$ one obtains $K^{(1)} = \nu_F |U_c| \ln(2\gamma E_F/\pi T)$, and

$$T_{c0} = \frac{2\gamma E_F}{\pi} \exp\left(-\frac{1}{\nu_F |U_c|}\right), \quad (29)$$

in agreement with Ref. [39] and with the usual BCS expression. We may now write

$$K_\sigma^{(1)} = 1 + \nu_F |U_c| \left[\ln \frac{T_{c0}}{T} + \pi T \sum_\omega \left(\left\langle \frac{\text{sign } \omega}{\omega + i\varepsilon_\sigma^+(\mathbf{k}, \mathbf{k} - \mathbf{Q})} \right\rangle_{k_y} - \frac{\text{sign } \omega}{\omega} \right) \right]. \quad (30)$$

The kernels $K_\sigma^{(1)}$ and $K_\sigma^{(3)c}$ can be further simplified in terms of the digamma function $\psi(x) = \frac{d}{dx} \ln \Gamma(x)$:

$$K_\sigma^{(1)} = 1 + \nu_F |U_c| \left[\ln \frac{T_{c0}}{T} + \psi\left(\frac{1}{2}\right) - \left\langle \text{Re } \psi\left(\frac{1}{2} + \frac{i\varepsilon_\sigma^+(\mathbf{k}, \mathbf{k} - \mathbf{Q})}{2\pi T}\right) \right\rangle_{k_y} \right], \quad (31)$$

$$K_\sigma^{(3)c} = -\frac{\nu_F |U_c|}{16\pi^2 T^2} \left\langle \text{Re } \psi''\left(\frac{1}{2} + \frac{i\varepsilon_\sigma^+(\mathbf{k}, \mathbf{k} - \mathbf{Q})}{2\pi T}\right) \right\rangle_{k_y}. \quad (32)$$

To actually find the fields $\Delta_{\mathbf{Q}\sigma}$ just below the transition point to the leading order, one has to make the substitution $K_\sigma^{(1)} \rightarrow K_\sigma^{(1)} - |\Delta_{\mathbf{Q}\sigma}|^2 K_\sigma^{(3)c}$ in (28). The ratio $\Delta_{\mathbf{Q}-} : \Delta_{\mathbf{Q}+}$ is real and at the transition point is the column ratio in (28),

$$\Delta_{\mathbf{Q}-} : \Delta_{\mathbf{Q}+} = \left(\frac{1+\nu}{2} K_+^{(1)} - 1 \right) : \left(\frac{\nu-1}{2} K_-^{(1)} \right) = \left(\frac{\nu-1}{2} K_+^{(1)} \right) : \left(\frac{1+\nu}{2} K_-^{(1)} - 1 \right). \quad (33)$$

Introducing the (real) ratio $\alpha \equiv |\Delta_{\mathbf{Q}-}|^2 : |\Delta_{\mathbf{Q}+}|^2$ we get

$$|\Delta_{\mathbf{Q}\sigma}^c|^2 = \frac{\alpha^{(1-\sigma)/2} \left(\nu K_+^{(1)} K_-^{(1)} - \frac{\nu+1}{2} (K_+^{(1)} + K_-^{(1)}) + 1 \right)}{K_+^{(3)c} \left(\nu K_-^{(1)} - \frac{\nu+1}{2} \right) + \alpha K_-^{(3)c} \left(\nu K_+^{(1)} - \frac{\nu+1}{2} \right)}. \quad (34)$$

The superscript "c" stands for the cosine phase. The CDW cosine phase with $q_x \neq 0$ was analyzed at the transition line by means of the susceptibility calculation and called the CDW_x phase, while the phase with $q_x = 0$ was called CDW₀²⁴.

4.. The Double Cosine Phase

Now we consider the solution with $\Delta_{\mathbf{Q}\sigma} \neq 0$ for $\mathbf{k} = \pm \mathbf{Q}_0 \pm \mathbf{q}$, where $\mathbf{Q}_0 = 2k_F \mathbf{e}_x + (\pi/b) \mathbf{e}_y$ and $q \ll k_F$. Strictly speaking, there exist no self-consistent solutions with only four harmonics present or all others damped by a factor of $\Delta_{\mathbf{Q}\sigma}/E_F$. However, the modulations given above have equal second-order transition temperatures, and immediately below the transition point other harmonics are damped by a factor of $\Delta_{\mathbf{Q}\sigma}/T$ or $\Delta_{\mathbf{Q}\sigma}/H$.

To obtain the leading-order expressions for the fields $\Delta_{\mathbf{Q}\sigma}$ in the vicinity of the transition line, we rewrite the

equations (12) in the "matrix" form

$$GG_0^{-1} - GF = I, \quad (35)$$

where

$$G(\mathbf{k}', \mathbf{k}) = g_\sigma(\mathbf{k}', \mathbf{k}), \quad G_0(\mathbf{k}', \mathbf{k}) = \frac{\delta(\mathbf{k}', \mathbf{k})}{i\omega - \varepsilon_\sigma(\mathbf{k})}, \quad (36)$$

$$F(\mathbf{k}', \mathbf{k}) = \sum_Q \Delta_{\mathbf{Q}\sigma} \delta(\mathbf{k}', \mathbf{k} - \mathbf{Q}).$$

The solution is

$$G = G_0 + G_0 F G_0 + G_0 F G_0 F G_0 + \dots \quad (37)$$

Omitting the contribution from the virtual states with the momentum $|k_x| \gtrsim 2k_F$, we obtain the consistency equation to the third order in $\Delta_{\mathbf{Q}\sigma}$:

$$\begin{aligned}
\Delta_{\mathbf{Q}_0+\mathbf{q},\sigma'} = & T \sum_{\mathbf{k}\omega\sigma} (U_c - U_s \sigma \sigma') \times \left[\frac{\Delta_{\mathbf{Q}_0+\mathbf{q},\sigma}}{(i\omega - \varepsilon_\sigma(\mathbf{k}))(i\omega - \varepsilon_\sigma(\mathbf{k} - \mathbf{Q}_0 - \mathbf{q}))} + \right. \\
& + \frac{\Delta_{\mathbf{Q}_0+\mathbf{q},\sigma} |\Delta_{\mathbf{Q}_0+\mathbf{q},\sigma}|^2}{(i\omega - \varepsilon_\sigma(\mathbf{k}))(i\omega - \varepsilon_\sigma(\mathbf{k} - \mathbf{Q}_0 - \mathbf{q}))(i\omega - \varepsilon_\sigma(\mathbf{k}))(i\omega - \varepsilon_\sigma(\mathbf{k} - \mathbf{Q}_0 - \mathbf{q}))} + \\
& + \frac{\Delta_{\mathbf{Q}_0+\mathbf{q},\sigma} |\Delta_{\mathbf{Q}_0-\mathbf{q},\sigma}|^2}{(i\omega - \varepsilon_\sigma(\mathbf{k}))(i\omega - \varepsilon_\sigma(\mathbf{k} - \mathbf{Q}_0 - \mathbf{q}))(i\omega - \varepsilon_\sigma(\mathbf{k} - 2\mathbf{q}))(i\omega - \varepsilon_\sigma(\mathbf{k} - \mathbf{Q}_0 - \mathbf{q}))} + \\
& \left. + \frac{\Delta_{\mathbf{Q}_0+\mathbf{q},\sigma} |\Delta_{\mathbf{Q}_0-\mathbf{q},\sigma}|^2}{(i\omega - \varepsilon_\sigma(\mathbf{k}))(i\omega - \varepsilon_\sigma(\mathbf{k} - \mathbf{Q}_0 + \mathbf{q}))(i\omega - \varepsilon_\sigma(\mathbf{k}))(i\omega - \varepsilon_\sigma(\mathbf{k} - \mathbf{Q}_0 - \mathbf{q}))} \right]. \tag{38}
\end{aligned}$$

The equation for the other two harmonics may be obtained via a substitution $\mathbf{q} \rightarrow -\mathbf{q}$. Performing the integration over k_x , we arrive at

$$\Delta_{\mathbf{Q}_0+\mathbf{q},\sigma'} = \sum_\sigma \frac{1 + \nu\sigma\sigma'}{2} \left(K_\sigma^{(1)} - |\Delta_{\mathbf{Q}_0+\mathbf{q},\sigma}|^2 K_\sigma^{(3)c} - |\Delta_{\mathbf{Q}_0-\mathbf{q},\sigma}|^2 K_\sigma^{(3)d} \right) \Delta_{\mathbf{Q}_0+\mathbf{q},\sigma} \tag{39}$$

(the superscript “d” stands for “double cosine”) with $K^{(1)}$ and $K^{(3)c}$ given by (31) and (32), and

$$\begin{aligned}
K_\sigma^{(3)d} = & \pi\nu_F |U_c| T \sum_\omega \left\langle \frac{(\omega - i\sigma H) \operatorname{sign} \omega}{[(\omega + i\varepsilon_\sigma^+(\mathbf{k}, \mathbf{k} - \mathbf{Q}))(\omega - i\varepsilon_{-\sigma}^+(\mathbf{k}, \mathbf{k} - \mathbf{Q}))]^2} \right\rangle_{k_y} = \\
= & -\frac{\nu_F |U_c|}{4\pi\hbar v_F q_x T} \left\langle \left[\operatorname{Im} \psi' \left(\frac{1}{2} + \frac{i\varepsilon_\sigma^+(\mathbf{k}, \mathbf{k} - \mathbf{Q})}{2\pi T} \right) + \operatorname{Im} \psi' \left(\frac{1}{2} + \frac{i\varepsilon_{-\sigma}^+(\mathbf{k}, \mathbf{k} - \mathbf{Q})}{2\pi T} \right) \right] \right\rangle_{k_y}. \tag{40}
\end{aligned}$$

The function $K_\sigma^{(3)d}$ does not depend on σ and in what follows we omit this subscript.

At only a longitudinal shift of the CDW wave vector ($q_y = 0$) the k_y -dependence of $\varepsilon_{-\sigma}^+(\mathbf{k}, \mathbf{k} - \mathbf{Q})$ is symmetric, and the functions $K_\sigma^{(1)}$, $K_\sigma^{(3)c}$ and $K^{(3)d}$ (being dependent only on the shift wave vector q_x) possess the symmetry:

$$\begin{aligned}
K_\sigma^{(1)}(q_x) &= K_{-\sigma}^{(1)}(-q_x), \\
K_\sigma^{(3)c}(q_x) &= K_{-\sigma}^{(3)c}(-q_x), \\
K^{(3)d}(-q_x) &= K^{(3)d}(q_x). \tag{41}
\end{aligned}$$

This symmetry follows directly from Eqs. (31), (32) and (40) and the properties of digamma function: $\operatorname{Re} \psi^{(n)}(a + ib) = \operatorname{Re} \psi^{(n)}(a - ib)$, $\operatorname{Im} \psi^{(n)}(a + ib) =$

$-\operatorname{Im} \psi^{(n)}(a - ib)$. This symmetry is not a consequence of the expansion in powers of Δ_σ : the consistency equation (22) also does not change under the transformation

$$q_x \rightarrow -q_x, \sigma \rightarrow -\sigma. \tag{42}$$

The ratio $|\Delta_{\mathbf{Q}_0+\mathbf{q},\sigma}|^2 : |\Delta_{\mathbf{Q}_0+\mathbf{q},-\sigma}|^2$ near the transition point is still given by (33) accounting for the property (41). Hence, $|\Delta_{\mathbf{Q}_0-\mathbf{q},\sigma}|^2 : |\Delta_{\mathbf{Q}_0-\mathbf{q},-\sigma}|^2 = |\Delta_{\mathbf{Q}_0+\mathbf{q},-\sigma}|^2 : |\Delta_{\mathbf{Q}_0+\mathbf{q},\sigma}|^2 \equiv \alpha$. As in derivation of (34) one may rewrite the system of equations (39) on Δ as two equations (28) with replacement $K_\sigma^{(1)}(\mathbf{Q}_0 \pm \mathbf{q}_x) \rightarrow K_{\pm\sigma}^{(1)} - |\Delta_{\mathbf{Q}_0 \pm \mathbf{q},\sigma}|^2 K_{\pm\sigma}^{(3)c} - |\Delta_{\mathbf{Q}_0 \mp \mathbf{q},\sigma}|^2 K^{(3)d}$.

Defining the ratio $\beta \equiv |\Delta_{\mathbf{Q}_0-\mathbf{q},-}|^2 : |\Delta_{\mathbf{Q}_0+\mathbf{q},+}|^2$ we can extend the derivation of (34) to get

$$|\Delta_{\mathbf{Q}_0+\mathbf{q},+}|^2 = \frac{\left(\nu K_+^{(1)} K_-^{(1)} - \frac{\nu+1}{2} (K_+^{(1)} + K_-^{(1)}) + 1 \right)}{\left(K_+^{(3)c} + \alpha\beta K^{(3)d} \right) \left(\nu K_-^{(1)} - \frac{\nu+1}{2} \right) + \left(\alpha K_-^{(3)c} + \beta K^{(3)d} \right) \left(\nu K_+^{(1)} - \frac{\nu+1}{2} \right)}, \tag{43}$$

and from the $\mathbf{Q}_0 - \mathbf{q}$ part of (39)

$$|\Delta_{\mathbf{Q}_0-\mathbf{q},-}|^2 = \frac{\beta \left(\nu K_+^{(1)} K_-^{(1)} - \frac{\nu+1}{2} (K_+^{(1)} + K_-^{(1)}) + 1 \right)}{\left(\beta K_+^{(3)c} + \alpha K^{(3)d} \right) \left(\nu K_-^{(1)} - \frac{\nu+1}{2} \right) + \left(\alpha\beta K_-^{(3)c} + K^{(3)d} \right) \left(\nu K_+^{(1)} - \frac{\nu+1}{2} \right)}. \tag{44}$$

Dividing (43) by (44) we obtain a linear equation on β :

$$\frac{(\beta K_+^{(3)c} + \alpha K^{(3)d}) (\nu K_-^{(1)} - \frac{\nu+1}{2}) + (\alpha \beta K_-^{(3)c} + K^{(3)d}) (\nu K_+^{(1)} - \frac{\nu+1}{2})}{(K_+^{(3)c} + \alpha \beta K^{(3)d}) (\nu K_-^{(1)} - \frac{\nu+1}{2}) + (\alpha K_-^{(3)c} + \beta K^{(3)d}) (\nu K_+^{(1)} - \frac{\nu+1}{2})} = 1, \quad (45)$$

which gives $\beta = 1$. The values $\beta = 0$ or $\beta = \infty$ in (43) and (44) correspond to cosine phase. Hence, in the double cosine phase the symmetry (42) is not broken, while the transition to cosine phase breaks this symmetry.

5.. Free energy of cosine and double-cosine phases

One can easily write down the expressions for the free energies of cosine and double-cosine phases valid to the second order in the energy gap $|\Delta_\sigma|$.

From (11) we have for the free energy

$$F_{\text{CDW}} - F_n = \frac{1}{2} \sum_{\mathbf{Q}\sigma} D_{-\mathbf{Q}\sigma} \Delta_{\mathbf{Q}\sigma}. \quad (46)$$

To the second order in $\Delta_{\mathbf{Q}\sigma}$ this rewrites as

$$\begin{aligned} F_{\text{CDW}} - F_n &= -\frac{\pi \nu_F T}{4} \sum_{\mathbf{Q}\omega\sigma} \left\langle \frac{\Delta_{\mathbf{Q}\sigma} \Delta_{-\mathbf{Q}\sigma} \text{sign } \omega}{\omega + i\varepsilon_\sigma^+(\mathbf{k}, \mathbf{k} - \mathbf{Q})} \right\rangle_{k_y} \\ &= -\frac{1}{4|U_c|} \sum_{\mathbf{Q}\sigma} K_\sigma^{(1)} |\Delta_{\mathbf{Q}\sigma}|^2. \end{aligned} \quad (47)$$

The phase with the most negative r.h.s of (46) wins; positive values of the r.h.s. correspond to first-order transitions. From Eq. (47) using Eq. (41) we have

$$F_c - F_n = -\frac{K_+^{(1)} + \alpha K_-^{(1)}}{2|U_c|} |\Delta_{\mathbf{Q}_0 + \mathbf{q}_x, +}^c|^2 \quad (48)$$

and

$$F_{2c} - F_n = -\frac{K_+^{(1)} + \alpha K_-^{(1)}}{|U_c|} |\Delta_{\mathbf{Q}_0 + \mathbf{q}'_x, +}^{2c}|^2. \quad (49)$$

The quantity $K_+^{(1)} + \alpha K_-^{(1)}$ depends on \mathbf{q} but is always positive near the metal-CDW transition line $T_c(H)$ where this transition is of the second kind.

Since CDW_c and CDW_{2c} phases have the same transition temperature, the only way to determine which phase takes place is to compare their free energies, that near the transition line $T_c(H)$ are given by the formulas (48) and (49). The double cosine phase wins if the ratio

$$r_F \equiv \frac{F_{2c} - F_n}{(F_c - F_n)} > 1, \quad (50)$$

where the values of the functions $F_{2c}(T, H, \mathbf{q})$ and $F_c(T, H, \mathbf{q})$ must be taken at the optimal value of the wave vector \mathbf{q} , that should be found by minimization of these free energy functions at each point of T, H phase diagram and for each of the two phases (CDW_c and CDW_{2c}) separately.

Below the transition temperature the optimal shift vectors \mathbf{q} could be different for the cosine and double cosine phases (they minimize different free energy functions F_c and F_{2c}). However, at the transition temperature $T_c(H)$ the CDW_c and CDW_{2c} phases have the same optimal value of \mathbf{q} which is determined by the minimum of the left-hand side of Eq. (28). Hence, on the transition line $T_c(H)$ Eq. (50) simplifies to

$$r_F = \frac{2|\Delta_{\mathbf{Q}_0 + \mathbf{q}_x, +}^{2c}|^2}{|\Delta_{\mathbf{Q}_0 + \mathbf{q}_x, +}^c|^2} > 1, \quad (51)$$

or after substitution of (34) and (43)

$$r_F = \frac{2 \left[K_+^{(3)c} \left(\nu K_-^{(1)} - \frac{\nu+1}{2} \right) + \alpha K_-^{(3)c} \left(\nu K_+^{(1)} - \frac{\nu+1}{2} \right) \right]}{\left(K_+^{(3)c} + \alpha K^{(3)d} \right) \left(\nu K_-^{(1)} - \frac{\nu+1}{2} \right) + \left(\alpha K_-^{(3)c} + K^{(3)d} \right) \left(\nu K_+^{(1)} - \frac{\nu+1}{2} \right)} > 1. \quad (52)$$

These formulas will be used later to determine the phase diagram.

III. THE PHASE DIAGRAM

In this section we only consider the longitudinal modulation ($q_y = 0$) of the CDW wave vector. The CDW phase with $q_y \neq 0$ (CDW_y phase) may appear for certain dispersion functions $t_\perp(\mathbf{k}_\perp)$. However, for the tight-

binding model (2) the CDW_y phase is not expected to take place near the transition temperature. Near the critical pressure (when $t'_b \approx t'^*_b$ and the SDW-metal phase transition takes place) in zero field the SDW_2 phase was predicted using the susceptibility calculation from the normal state.⁴⁰ However, this phase was predicted only near $T = 0$. Moreover, the absolute instability line calculated in [40] does not give the actual transition line at low temperature since this transition takes place as the first-order phase transition.

To be more sure that we can disregard appearance of the CDW_y phase in our consideration near the transition temperature we performed the calculation of the optimal shift vector \mathbf{q} at the transition line $T_c(H)$ in a large range of parameters. We swept the following three-dimensional range of parameters: $-0.3 \leq \nu \leq 0.9$, $0 \leq t'_b/t'^*_b < 1$ and $0 \leq \mu_B H \leq 2T_{c0}$ and have not found that the shift of Q_y leads to higher T_c anywhere inside this range.

This does not contradict the prediction of the CDW_y ²⁴, since according to this paper the CDW_y phase appears at $\nu < 0$ essentially due to the orbital effect of the magnetic field (see Fig. 7d of Ref. [24]). Below we will only consider the range $0 \leq \nu < 1$ which is close to the experimental situation in organic metals and disregard the appearance of CDW_y phase.

1.. Transition line $T_c(H)$ and the normal- CDW_0 - CDW_x tricritical point

The normal-to-CDW phase transition line is given by Eq. (28) irrespective of to which CDW phase this transition occurs. The shift of the wave vector q_x which enters Eq. (28) corresponds to the maximum value of T_c at given magnetic field H . The behavior of $T_c(H)$ and $q_x(H)$ at the transition temperature has been analyzed in Ref. [24]. Diagonalization of the M_3, M_4 part of the susceptibility matrix (6) in Ref. [24] corresponds to the diagonalization of the matrix in Eq. (28). On the transition line one of the eigenvalues of these matrices is zero. In the case of perfect nesting equation (28) gives the same result for $T_c(H)$ as Eq. (17) of Ref. [24] (see fig. 7(a) of [24]).

For $q_x = 0$ (CDW_0 phase) $K_+^{(1)} = K_-^{(1)}$ and Eq. (28) simplifies to $K_+^{(1)} = 1$, that gives for the transition temperature $T_c = T_c(H)$ the well-known equation

$$\ln \left(\frac{T_c(H, t'_b)}{T_{c0}} \right) = \psi \left(\frac{1}{2} \right) - \left\langle \text{Re } \psi \left(\frac{1}{2} - \frac{i\varepsilon_\sigma^+(\mathbf{k}, \mathbf{k} - \mathbf{Q}_0)}{2\pi T_c} \right) \right\rangle_{k_y}, \quad (53)$$

where

$$\varepsilon_\sigma^+(\mathbf{k}, \mathbf{k} - \mathbf{Q}_0) = -2t'_b \cos(2k_y b) - \sigma H. \quad (54)$$

In the Eq. (53) one can take either of the values $\sigma = \pm 1$ since this equation does not depend on the sign of σ . The transition line $T_c(H)$ from normal to CDW_0 phase does not depend on the value of ν .

The tricritical point (where the CDW_0 and CDW_x phases have the same transition temperature) is given by equation $\partial^2 D(\nu, T, H, q_x)/\partial q_x^2 = 0$, where $D(\nu, T, H, q_x)$ is the left-hand side of Eq. (28). At this point $q_x = 0$, $\Rightarrow K_+^{(1)} = K_-^{(1)} = 1$ and $\partial^n K_+^{(1)}/\partial q_x^n = (-1)^n \partial^n K_-^{(1)}/\partial q_x^n$, and the equation for the tricritical point becomes

$$\frac{\partial^2 K^{(1)}}{(\partial q_x)^2} = -\frac{2\nu}{1-\nu} \left(\frac{\partial K^{(1)}}{\partial q_x} \right)^2. \quad (55)$$

Substituting (31) and (32) this equation rewrites as

$$-\left\langle \text{Re } \psi'' \left(\frac{1}{2} - \frac{i\varepsilon_\sigma^+(\mathbf{k}, \mathbf{k} - \mathbf{Q}_0)}{2\pi T_c} \right) \right\rangle_{k_y} = \eta \left[\left\langle \text{Im } \psi' \left(\frac{1}{2} - \frac{i\varepsilon_\sigma^+(\mathbf{k}, \mathbf{k} - \mathbf{Q}_0)}{2\pi T_c} \right) \right\rangle_{k_y} \right]^2, \quad (56)$$

where

$$\eta = 2\nu\nu_F|U_c|/(1-\nu). \quad (57)$$

Together with Eq. (53) this equation allows to find the tricritical point.

2.. $T_c(H)$ transition line at perfect nesting

The case of perfect nesting ($t'_b = 0$) is equivalent to the strictly 1D case in many mathematical aspects. However, the 3D nature of the compound (its energy spectrum, e-e interaction and lattice elasticity) preserves, and the mean-field approach still works. The analysis in this subsection (at $t'_b = 0$) is simple and performed analytically. It helps to understand some qualitative features of the CDW phase diagram in magnetic field.

At perfect nesting and purely longitudinal modulation of CDW ($q_y = 0$) the expressions for $K_\sigma^{(1)}$, $K^{(3)d}$ and $K_\sigma^{(3)c}$ simplify to

$$K_{\sigma 0}^{(1)} = 1 + \nu_F |U_c| \left[\ln \frac{T_{c0}}{T} + \psi \left(\frac{1}{2} \right) - \operatorname{Re} \psi \left(\frac{1}{2} + \frac{i h_\sigma}{2\pi T} \right) \right], \quad (58)$$

$$K_0^{(3)d} = -\frac{\nu_F |U_c|}{4\pi \hbar v_F q_x T} \left[\operatorname{Im} \psi' \left(\frac{1}{2} + \frac{i h_\sigma}{2\pi T} \right) + \operatorname{Im} \psi' \left(\frac{1}{2} + \frac{i h_{-\sigma}}{2\pi T} \right) \right], \quad (59)$$

and

$$K_{\sigma 0}^{(3)c} = -\frac{\nu_F |U_c|}{16\pi^2 T^2} \operatorname{Re} \psi'' \left(\frac{1}{2} + \frac{i h_\sigma}{2\pi T} \right), \quad (60)$$

where

$$h_\sigma = \frac{\hbar v_F q_x}{2} - \sigma H. \quad (61)$$

At $q_x = 0$, Eq. (59) even more simplifies:

$$K_{00}^{(3)d} = -\frac{\nu_F |U_c|}{8\pi^2 T^2} \operatorname{Re} \psi'' \left(\frac{1}{2} - \frac{i H}{2\pi T} \right) = 2K_{\sigma 00}^{(3)c}. \quad (62)$$

One can now derive a simple formula for the transition line $T_c(H)$ in the high field limit $H \gg T_c(H)$. As $H \rightarrow \infty$, h_σ in (61) goes to zero for one spin component and to $-2\sigma H$ for the other. Using the limit expansion of the digamma function, $\operatorname{Re} \psi(1/2 + ix) = \ln x + O(1/x)$, $x \rightarrow \infty$, from (58) we have at $H/\pi T_c(H) \gg 1$

$$\begin{aligned} K_+^{(1)} &\approx 1 + \nu_F |U_c| \ln(T_{c0}/T) \\ K_-^{(1)} &\approx 1 + \nu_F |U_c| \ln(\pi T_{c0}/4\gamma H). \end{aligned} \quad (63)$$

Equation (28) rewrites as

$$K_+^1 = \frac{(1 + \nu) K_-^{(1)}/2 - 1}{\nu K_-^{(1)} - (1 + \nu)/2},$$

that in the limit $H/\pi T_c(H) \gg 1$ becomes

$$\ln(T_{c0}/T) = \frac{\ln(4\gamma H/\pi T_{c0})}{\eta \ln(4\gamma H/\pi T_{c0}) + 1}. \quad (64)$$

At $\eta \ln(4\gamma H/\pi T_{c0}) \gg 1$ this simplifies to

$$T_c(H \rightarrow \infty) = T_{c0} \exp(-1/\eta). \quad (65)$$

In the intermediate interval $\pi T_c(H) \ll 4\gamma H \ll \pi T_{c0} \exp(1/\eta)$ we get

$$T_c(H) \approx \pi T_{c0}^2 / (4\gamma H). \quad (66)$$

Hence, at perfect nesting in the limit $H \rightarrow \infty$ the transition temperature tends to a finite value which is natural since it corresponds to the CDW instability for only one spin component.

However, the behavior of $T_c(H)$ given by formulas (64), (65) and (66) strongly changes at finite "antnesting" term t'_b (see below).

3.. Metal-CDW transition lines and tricritical points at finite t'_b

Using the Eq. (28) and Eq. (56) we calculated the transition lines $T_c(H)$ and the tricritical points at different values of t'_b and ν . The results are shown in Fig. 1. From this figure we see that the transition line $T_c(H)$ depends strongly on the both parameters t'_b and ν , and one cannot determine the value of t'_b from the $T_c(H)$ transition line if one does not know the value of ν . Hence, to determine experimentally what values take t'_b and ν in a particular compound, one has to perform two independent tests. For example, one can study the pressure dependence of the $T_c(H)$ lines at two different tilt angles of magnetic field: the first measurement when the magnetic field is parallel to the conducting x - y plane and the formulas derived above in neglect of orbital effects are valid, the second measurement in the very strong magnetic field perpendicular to the conducting x - y plane, when the orbital effects are so strong that the one-dimensionization of the electron dispersion takes place and the formulas for perfect nesting (see sec. 3.2) become approximately valid. One can also determine the value of t'_b independently from the transport measurement and then compare it to the critical value of $t_b^* = \Delta_0/2 \approx 0.88 T_{c0}$ at which the CDW state is damped without magnetic field.

There is one interesting common feature on all diagrams in Figs. 1. At each value of ν there is a critical value of $t'_b < t_b^*$ above which the CDW_x phase disappears, i.e. as magnetic field increases the transition from CDW_0 to metal state instead of the CDW_x phase takes place up to the lowest temperature. This critical value of t'_b may shift due to the "one-dimensionization" effect of magnetic field.

We have also checked if the region of cosine phase increases considerably after finite "antnesting" term is taken into account. The results of this study at the transition line are given in Fig. 2. These results indicate that the region of cosine phase does not increase considerably at finite t'_b for the tight-binding dispersion.

4.. Cosine and double-cosine phases at perfect nesting

To determine which of the two phases (CDW_c or CDW_{2c}) wins we have to compare their free energies given in section 2.5.

On the transition line this reduces to the evaluation of the ratio (52). At the tricritical point (when $q_x = 0$) this

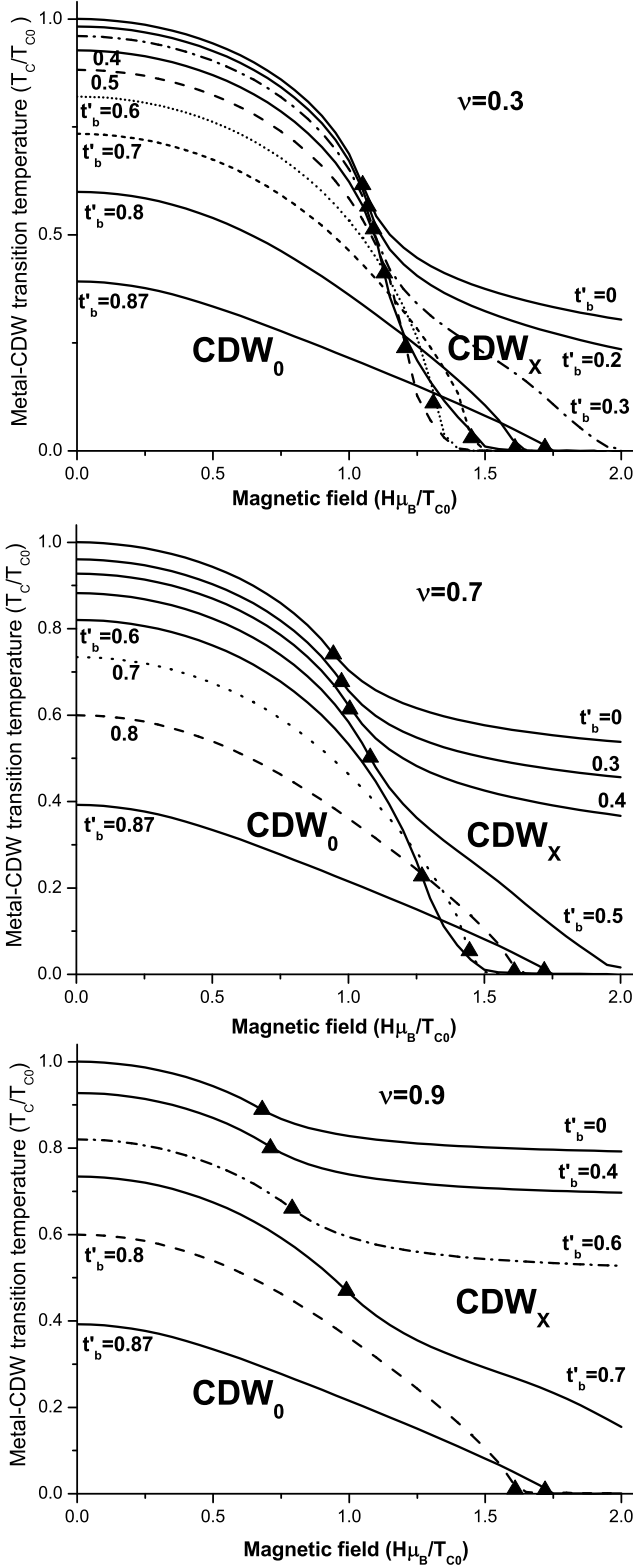


FIG. 1: Transition lines $T_c(H)$ at different values of t'_b at three different values of the coupling constant ratio ν . The values of t'_b are given on the figures in units of T_{c0} ; for the tight-binding dispersion (2) the critical value of t'_b at which CDW disappears without magnetic field is $t_b^* = \Delta_0/2 \approx 0.88T_{c0}$. The triangles show the tricritical points Normal-CDW₀-CDW_X.

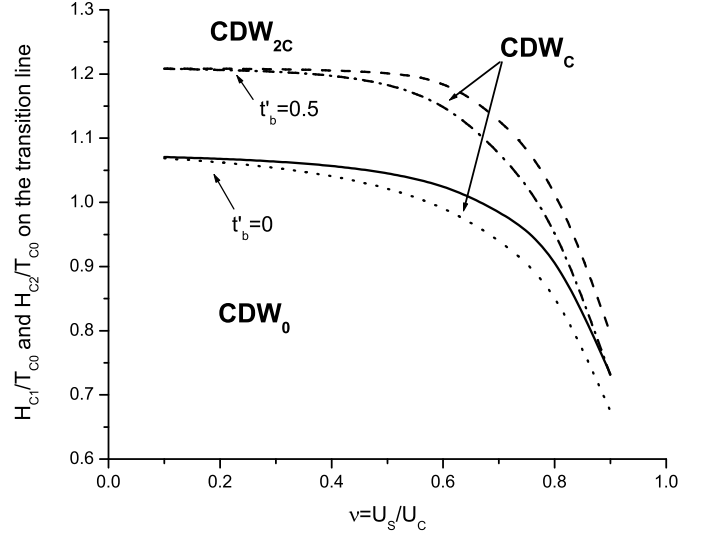


FIG. 2: The magnetic field values $H_{c1}(\nu)$ and $H_{c2}(\nu)$ at two tricritical points Normal-CDW₀-CDW_c and Normal-CDW_c-CDW_{2c} correspondingly as function of coupling constant ratio $\nu = U_s/U_c$ for two different values of t'_b . The solid and dot lines denote $H_{c2}(\nu)$ and $H_{c1}(\nu)$ at perfect nesting ($t'_b = 0$) while the dash and dash-dot lines denote $H_{c2}(\nu)$ and $H_{c1}(\nu)$ at finite value of the "antinesting" term ($t'_b = 0.5T_{c0}$). The cosine phase exists in the areas between $H_{c1}(\nu)$ and $H_{c2}(\nu)$ lines at the same value of t'_b .

ratio can be easily evaluated using Eq. (62):

$$r_{F\text{triple}} = 2/3 < 1. \quad (67)$$

Hence, near the tricritical point the cosine phase wins. In the limit of high field ($H \gg T_c$) one has $\hbar v_F q_x \rightarrow 2H$ and $h_\sigma \rightarrow (1 - \sigma)H$. In this limit $K_+^{(3)c} \approx -(\nu_F|U_c|/16\pi^2T^2) \text{Re } \psi''(1/2) \gg K_-^{(3)c}, K^{(3)d}$, and from (52) we get

$$r_F \rightarrow 2 \text{ at } H/T_c \rightarrow \infty. \quad (68)$$

Hence, at high magnetic field the double cosine phase wins. These two simple estimates suggest that the cosine and double-cosine phases both appear on the phase diagram.

The boundary between CDW_c and CDW_{2c} phases on the transition line $T_c(H)$ is given by the equation $r_F(T, H, \nu) = 1$, which rewrites as

$$\begin{aligned} & \left(K_+^{(3)c} - \alpha K^{(3)d} \right) \left(\nu K_-^{(1)} - \frac{\nu + 1}{2} \right) = \\ & = \left(K^{(3)d} - \alpha K_-^{(3)c} \right) \left(\nu K_+^{(1)} - \frac{\nu + 1}{2} \right). \end{aligned} \quad (69)$$

This equation is valid also for nonzero t'_b and together with Eq. (28) allows to determine the second tricritical point $(H_{c2}(\nu), T_c(H_{c2}))$ where the normal, CDW_c and CDW_{2c} phases meet.

In Fig. 2 we plot two triple-point values $H_{c1}(\nu)$ and $H_{c2}(\nu)$ of magnetic field which are given by equations

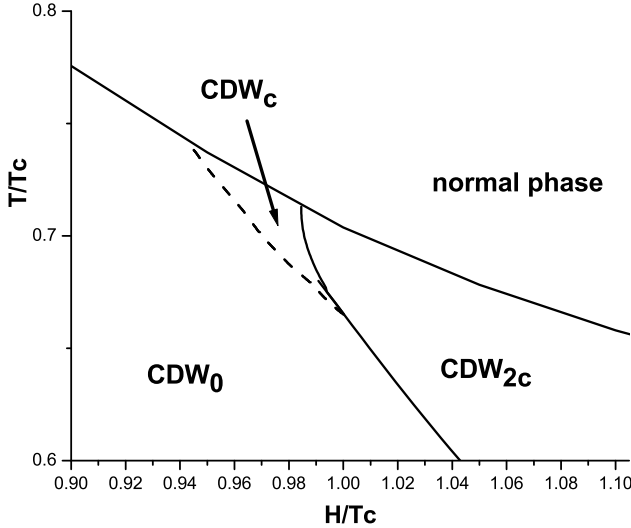


FIG. 3: Phase diagram in $H - T$ coordinates at $\nu = 0.7$ at perfect nesting near the tricritical point. The CDW_c region disappears rapidly as temperature decreases below T_c .

(56) and (69) correspondingly (together with Eq. (28)) at two different values of $t'_b = 0$ and $t'_b = 0.5T_{c0}$. $H_{c1}(\nu)$ and $H_{c2}(\nu)$ determine the tricritical points Normal- CDW_0 - CDW_c and Normal- CDW_c - CDW_{2c} . From this figure we see that the range of the cosine phase is very narrow (the difference $H_{c2} - H_{c1}$ does not exceed 5% of H_{c1}) and strongly depends on ν .

At perfect nesting two tricritical points H_{c1} and H_{c2} coincide at $\nu = 0$. At this "double-triple" point the denominator in formulas (34) and (43) is zero. This means, that one should expand up to the higher orders in $|\Delta^2|$ than fourth and that at this point the critical fluctuations are very strong.

From Fig. 2 we see that (i) on the phase diagram of CDW in magnetic field there are at least 3 different CDW states: CDW_0 , CDW_c and CDW_{2c} , (ii) at the transition line $T_c(H)$ the region of the CDW_c phase is quite narrow for various values of t'_b and is usually sandwiched between the CDW_0 and CDW_{2c} phases as the magnetic field increases.

To analyze how this picture evolves below the transition line $T_c(H)$ we performed a numerical calculation of the free energies of CDW_c and CDW_{2c} phases using formulas (48),(49),(43),(34). These formulas are valid if $\Delta \ll \pi T, H$, that covers a narrow region below $T_c(H)$.

The computation performed in the case of perfect nesting shows that the region of the CDW_c phase becomes even more narrow as the temperature decreases and disappears at $T \approx 0.95T_c(H)$ (see Fig. 3). Hence, the cosine phase at perfect nesting exists only in a very small region of the phase diagram where it is strongly smeared by the critical fluctuations.

The similar phase diagram appears in surface superconductors in parallel magnetic field.⁴¹ The cosine and double-cosine CDW phases correspond to the helical and cosine (stripe) superconducting phases respectively, and

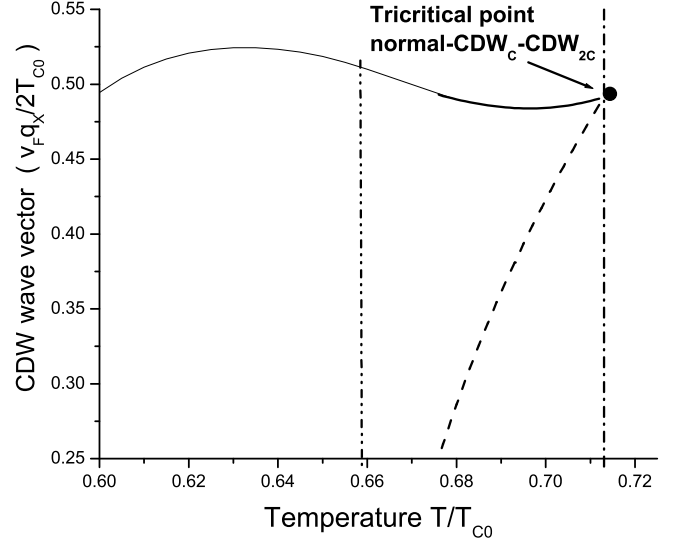


FIG. 4: The shifts q_x of wave vectors of the phases CDW_{2c} (solid line) and CDW_c (dash line) along the CDW_c - CDW_{2c} transition line (at $0.713 > T/T_{c0} > 0.66$) or CDW_0 - CDW_{2c} transition line (at $T/T_{c0} < 0.66$) as function of temperature. These shifts coincide only at the normal- CDW_c - CDW_{2c} tricritical point at $T/T_{c0} = 0.713$. The difference between the solid and dash lines gives the jump of the CDW wave vector on the CDW_c - CDW_{2c} transition line that makes this transition of the first kind and leads to hysteresis. The dash-dot line stands for the normal-CDW transition temperature, and the dash-double-dot line shows the temperature of CDW_0 - CDW_{2c} tricritical point.

the total CDW_x phase corresponds to the non-uniform superconducting LOFF state.^{8,9} However, our situation differs from that in Ref. [41], where the Rashba term in the electron dispersion relation plays an important role in obtaining the phase diagram similar to that on Fig. 3. The number of harmonics and coupling constant in our case is twice larger than that in Ref. [41]. However, the analogy between CDW and surface superconductors in magnetic field is rather deep (see the discussion section).

On the transition line CDW_c - CDW_{2c} the energy gaps and the optimal shifts q_x of the CDW wave vectors of these two phases become substantially different as the temperature decreases below T_c (see Figs. 4). This means that the transition from CDW_c to CDW_{2c} is of the first order. The transition line between CDW_0 and CDW_{2c} is also of the first order, and the CDW_{2c} nesting vector differs from $Q_0 = 2k_F$ already on the transition line (see Fig. 4). This fact explains the huge hysteresis in magnetization and magnetoresistance observed in α -(BEDT-TTF)₂KHg(SCN)₄ at the kink transition.^{29,30,32} The first-order phase transition driven by magnetic field is usually accompanied by hysteresis. The jump of the nesting vector on the CDW_0 - CDW_{2c} transition line itself leads to huge hysteresis. The CDW and its wave vector are pinned by the impurities and crystal imperfections.¹ As magnetic field increases through the kink transition point $H = H_c(T)$, the jump of the CDW wave vector forces the CDW condensate to move. Due to the pinning

this motion is hysteretic since at each time moment the CDW condensate finds some local minimum of the impurity potential. The larger jump of the CDW wave vector at the kink transition the greater the hysteresis is. This jump decreases with increasing temperature and comes to zero on the transition line $T_c(H)$. The hysteresis shows a similar temperature dependence. The hysteresis reduces with heating also due to the thermal activation processes which reduce the pinning.

IV. DISCUSSION

The electron charge and spin densities and the lattice distortion differ considerably in the cosine CDW_c and double-cosine CDW_{2c} phases that can help to distinguish these two states experimentally. In the double-cosine phase the charge modulation is the sum of two cosine distortions that leads to the beats of the charge density wave:

$$\begin{aligned}\rho_C^{2c}(x) &= \nu_F(\Delta_+ + \Delta_-)\{\cos[(Q_0 + q_x)x + \phi_1] \\ &\quad + \cos[(Q_0 - q_x)x + \phi_2]\} \\ &= 2\nu_F(\Delta_+ + \Delta_-)\cos[Q_0x + (\phi_1 + \phi_2)/2] \\ &\quad \times \cos[q_xx + (\phi_1 - \phi_2)/2].\end{aligned}\quad (70)$$

The phase shifts ϕ_1 and ϕ_2 may depend on coordinate because of the pinning of CDW by impurities. Usually, $\Delta_+(Q)$ and $\Delta_-(Q)$ in CDW_{2c} state differ substantially, and the charge density wave in magnetic field is accompanied by a spin density wave. The spin-density modulation in the double-cosine phase is given by

$$\begin{aligned}\rho_S^{2c}(x) &= \nu_F(\Delta_+ - \Delta_-)\{\cos[(Q_0 + q_x)x + \phi_1] \\ &\quad - \cos[(Q_0 - q_x)x + \phi_2]\} \\ &= -2\nu_F(\Delta_+ - \Delta_-)\sin[Q_0x + (\phi_1 + \phi_2)/2] \\ &\quad \times \sin[q_xx + (\phi_1 - \phi_2)/2].\end{aligned}\quad (71)$$

In the cosine phase both charge and spin densities have one-cosine modulations,

$$\begin{aligned}\rho_C^c(x) &= \nu_F(\Delta_+ + \Delta_-)\cos[(Q_0 + q_x)x + \phi_1] \\ \rho_S^c(x) &= \nu_F(\Delta_+ - \Delta_-)\cos[(Q_0 + q_x)x + \phi_1].\end{aligned}\quad (72)$$

Thus, the charge modulations in the cosine and double-cosine phases can be experimentally distinguished by X-ray or Raman scattering, and the spin modulation can be detected by muon or neutron scattering experiments.

The energy spectrum in the cosine and double-cosine phases also differ strongly. In the cosine phase the energy spectrum (19) is asymmetric with respect to the spin components since the energy gaps Δ_σ differ for two spin components σ . This means that under external electric field the spin current is produced in addition to the charge current since the charge is transferred by electrons with predominantly one spin component. The degree of current polarization depends on the shift of CDW wave vector, and, hence, can be controlled by the external magnetic field. This property of the cosine phase may

find applications in spintronics. The double-cosine phase is symmetric in spin components, and its energy spectrum has at least two gaps for each spin component. The symmetry (42) preserves in the double-cosine phase while in the cosine phase it is spontaneously broken. Thus, the one-cosine and double-cosine CDW states differ substantially in their thermodynamic, transport and optical properties.

At low temperature $T \ll T_c$ the expansion in (37) is not applicable and the additional harmonics $\mathbf{Q} + (2n + 1)\mathbf{q}_x$ with integer n appear in the double-cosine solution of the consistency equation. These harmonics make the charge modulation in the CDW_{2c} phase at low temperature essentially nonsinusoidal in space and, possibly, containing soliton walls. At low temperature the quasi-particles differs substantially from the pair excitations with activation energy 2Δ suggested by the simple mean-field description. Even at finite inter-chain electron dispersion the variational methods using the soliton solutions of the consistency equations show¹⁶ that the lowest-energy excitations do not resemble the one-electron-type quasi-particles but involve many electrons and are accompanied by a "soliton" kinks in the coordinate dependence of the order-parameter $\Delta_\sigma(x)$. These excitations in the incommensurate CDW have spin 1/2, zero charge and the energy $2\Delta/\pi$ for a 1D chain without magnetic field. In external magnetic field their activation may become energetically favorable at $H > 2\Delta_0/\pi^{17}$ that corresponds to the phase-transition from CDW_0 to the CDW_x phase. Unfortunately, there is no a complete solution of this problem at nonzero temperature at present time. The calculation at the electron density close to half-filling²⁵ does not describe properly the incommensurate case far from the half-filling. In particular, it considers only the one-cosine modulation of the charge density. As we have seen, it is usually energetically less favorable than the double-cosine phase in high magnetic field. Therefore, we do not present an exact phase diagram in the whole temperature and magnetic field range.

Qualitatively, for the tight-binding dispersion one may expect the following picture. The cosine phase does not appear on the phase diagram besides the small region near the tricritical point as shown on Fig. 3. One can easily show that in the case of perfect nesting at $T \rightarrow 0$ the cosine phase is always unstable toward the formation of the double-cosine modulation. However, an observation of the cosine phase would be very interesting because of its spin asymmetry in thermodynamic and transport properties. For this reason some further calculation of the phase diagram for various electron dispersion relations would be interesting. The transition from CDW_0 to CDW_{2c} phase at low temperature comes about as the appearance of soliton kinks (or soliton walls).¹⁷ The soliton phase described in Ref. [17] has two forbidden bands (energy gaps) which makes it similar to the double-cosine phase. With increase of magnetic field the density of kinks increases, and the order parameter comes continuously to the sinusoidal modulation close to that in the double-cosine phase. At perfect nesting the

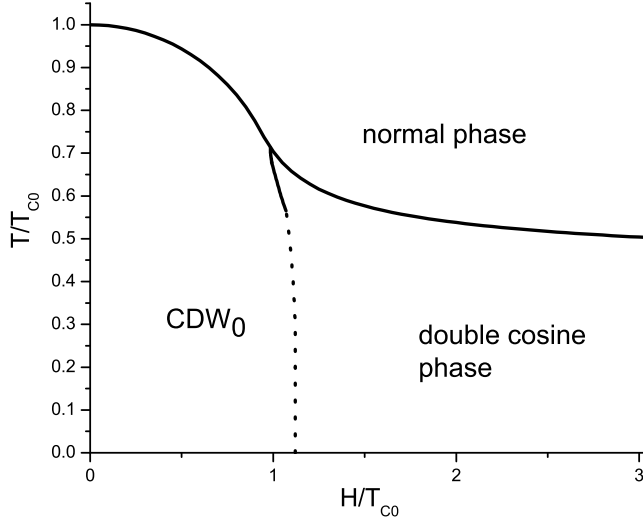


FIG. 5: Phase diagram in $H-T$ coordinates at perfect nesting in the whole essential region of CDW at $\nu = 0.7$. The solid lines have been calculated from Eqs. (28), (48), (49), (34) and (43). The CDW_c region is so narrow that it can hardly be distinguished on the total phase diagram. The dot line is a smooth link between the CDW_0 - CDW_{2c} boundary near T_c and its value $H_c = 2\Delta_0/\pi \approx 1.12T_{c0}$ at $T = 0$.

CDW_0 - CDW_{2c} boundary may be obtained qualitatively at arbitrary temperature as a smooth link between Fig. 3 and the point $H_c = 2\Delta_0/\pi \approx 1.1T_{c0}$ (see Fig. 5).

In the case of non-uniform LOFF state the susceptibility calculation in metal phase only gives the length of the optimal wave vector $|\mathbf{q}_{opt}|$ of the order-parameter modulation. To determine the most energetically favorable combination of \mathbf{q} : $|\mathbf{q}| = |\mathbf{q}_{opt}|$ one has to consider the third-order terms in $|\Delta|$ in the consistency equation. To determine which phase, CDW_c or CDW_{2c} , wins we performed the similar procedure. Our procedure takes into account some peculiarities of the CDW state such as the influence of the "antinesting" harmonic in the electron dispersion.

We have already mentioned the resemblance of the phase diagram obtained for CDW (Fig. 3) with that of layered superconductors with Rashba term.⁴¹ The CDW_0 - CDW_{2c} transition at low temperature also has many common features with the transition from uniform superconducting state to LOFF state in layered superconductors.⁴² In that case at the first critical field H_{c1} the formation of a single soliton kink also becomes energetically favorable, and the functional shape of this soliton is well approximated by $\Delta(x) = \Delta_0 \tanh(x/x_0)$ both in CDW_{2c} and LOFF states at low temperature. However, there are some important differences between these two systems. In the case of superconductivity the phase transition to the LOFF state was predicted to be of the second kind⁴², and the concentration of soliton walls increases gradually from zero with the increase of the magnetic field. In Ref. [17] the first-order phase transition was predicted between the uniform CDW and soliton phases. Our calculation also suggests

the first-order transition between CDW_0 and CDW_{2c} phases. The first-order phase transition from metal to the LOFF phase was predicted by both the mean-field⁴² and renormalization-group studies.⁷ The renormalization group analysis suggests⁷ that the enhanced fluctuations of the LOFF state, associated with additional broken symmetries, are important to make this transition of the first order. We do not consider the effect of fluctuations. According to the criterion in Refs. [5,6] the effects of fluctuations must not destroy the mean-field solution in organic metals where the interlayer transfer integral t_b is, usually, much larger than T_{c0} . The transition from the normal state to the CDW_x phase observed on experiments²⁶⁻³⁶ seems also to be of the second order. Further analysis of the CDW_0 - CDW_x phase diagram in the case of imperfect nesting at other dispersion relation can give more accurate description and even new qualitative features.

Our results are aimed to help to analyze the rather complicated phase diagram of CDW state in high magnetic field observed in a number of organic metals, such as α -(BEDT-TTF)₂KHg(SCN)₄²⁶⁻³⁴ (see also a discussion in [38]), $(Per)_2M(mnt)_2$ (M being Au, Pt, Cu)³⁵⁻³⁷ etc, where the transition from CDW_0 to high-field CDW_x phase is within the experimentally achievable magnetic fields. The above investigation may also be applied to analyze the phase diagram in nonorganic compounds with CDW ground state² (the attainable magnetic field in pulsed magnets is already comparable to the transition temperatures in some of these compounds). An accurate quantitative description and comparison with the experimental observations in Refs. [26-36] may require the substitution of a more realistic electron dispersion relation for each compound in the formulas derived above. With the two-harmonic tight-binding dispersion our study already explains several qualitative features of the CDW state in high magnetic field. First, we show that the transition from CDW_0 to CDW_x state is of the first kind and is accompanied by the substantial jumps of the energy gap in electron spectrum and of the nesting vector that results in strong hysteresis. This fact being observed in many experiments on α -(BEDT-TTF)₂KHg(SCN)₄ has not received a theoretical substantiation before. Second, we propose and prove the appearance of double-cosine CDW above the kink field which is consistent with the low temperature soliton solution. Third, we describe some properties of the cosine and double-cosine phases.

To summarize, we have developed a mean-field theory of the CDW state in magnetic field which takes into account imperfect nesting and the shift of the CDW wave vector. This allows a detailed study of the CDW properties and the phase diagram in high magnetic field below the transition temperature. Our analysis gives the link between the previous theoretical results based on the susceptibility calculation²⁴ and the soliton solutions at zero temperature.^{16,17} Although our study of the CDW_{2c} state is only applicable close to the transition line $T_c(H)$ where the ratio Δ_σ/T_c can be considered as a small parameter, even an investigation in this region allows

to make some important conclusions about the structure of CDW at high magnetic field. We have shown that the CDW_x state at high magnetic field has predominantly a double-cosine modulation with wave vectors $\mathbf{Q}_\pm = \mathbf{Q}_0 \pm \mathbf{q}_x$. At perfect nesting the one-cosine CDW with shifted wave vector exists (according to the mean-field calculations) only in a very narrow region near the tricritical point (see Fig. 3 and Fig. 5). The finite second ("antinesting") harmonic in the electron dispersion (2) does not change this picture considerably. However,

more specific dispersions or other perturbations may substantially change the phase diagram. We also suggest an interesting peculiarity of the cosine phase — its spin asymmetry that allows to make a controllable spin current.

P.G. is grateful to L.P. Gor'kov and M.V. Kartsovnik for many useful discussions and to A. Melikidze for critical reading. The work was supported by (PG) NSF Cooperative agreement No. DMR-0084173 and the State of Florida, and, in part, by INTAS No 01-0791 and RFBR.

^{*} Permanent address: L. D. Landau Institute for Theoretical Physics, Chernogolovka, Russia; Electronic address: grigorev@magnet.fsu.edu

¹ G. Grüner, *Density waves in Solids* Perseus Publishing; 1st edition (January 15, 2000).

² P. Monceau, *Electronic Properties of Inorganic Quasi One-Dimensional Compounds*, D. Reidel Pub. Co.; (April 2002).

³ See e.g., the books: E. Fradkin, *Field Theories of Condensed Matter Systems*, Westview Press (March, 1998); Alexander O. Gogolin, Alexander A. Nersesyan, Alexei M. Tsvelik, *Bosonization Approach to Strongly Correlated Systems*, Cambridge University Press (December 10, 1998).

⁴ One illustrating example that the strictly 1D models are not applicable to describe actual Q1D compounds could be the phase diagram of low-temprature ground state in coordinates of coupling constants. The renorm-group solution of the 1D models with $g_{1,2}$ coupling constants (g_1 and g_2 being the backward and forward scattering amplitudes respectively) (see, e.g., D. Senechal, cond-mat/9908262) gives the gapless Luttinger-liquid state at $|g_1| < 2g_2$ while in actual compounds no such a state is usually observed.

⁵ B. Horovitz, H. Gutfreund and M. Weger, Phys Rev B. **12**, 3174 (1975)

⁶ Ross H. McKenzie, Phys Rev B. **52**, 16428 (1995)

⁷ T. Ishiguro, K. Yamaji, and G. Saito, *Organic Superconductors*, 2nd edition, Springer-Verlag Berlin Heidelberg, 1998.

⁸ P. Fulde and A. Ferrel, Phys. Rev. 135, A550 (1964).

⁹ A. I. Larkin and Yu. N. Ovchinnikov, Sov. Phys. JETP 20, 762 (1965).

¹⁰ W.P. Su, J. R. Schrieffer and A. J. Heeger, Phys. Rev. Lett. **42**, 1698 (1979); Phys. Rev. B **22**, 2099 (1980).

¹¹ S.A. Brazovskij, Sov. Phys. JETP **51**, 342 (1980).

¹² S.A. Brazovskii, L.P. Gor'kov, J.R. Schrieffer, Physica Scripta **25**, 423 (1982).

¹³ S.A. Brazovskii, L.P. Gor'kov, A.G. Lebed', Sov. Phys. JETP **56**, 683 (1982) [Zh. Eksp. Teor. Fiz. **83**, 1198 (1982)].

¹⁴ A.I. Buzdin and V.V. Tugushev, Sov. Phys. JETP **58**, 428 (1983) [Zh. Eksp. Teor. Fiz. **85**, 735 (1983)].

¹⁵ W.P. Su and J. R. Schrieffer, *Physics in One Dimension*, Ed. by J. Bernasconi and T. Schneider, Springer series in Solid State Sciences, Berlin, Heidelberg and New York: Springer, 1981.

¹⁶ S.A. Brazovskij and N.N. Kirova, Sov. Sci. Rev. A Phys., volume **5**, p. 99 (1984).

¹⁷ S.A. Brazovskii, I.E. Dzjaloshinskii and N.N. Kirova, Sov. Phys. JETP **54**, 1209 (1981) [ZhETF 81, 2279 (1981)].

¹⁸ L. P. Gor'kov and A. G. Lebed, J. Phys. (Paris) Lett. **45**, L433 (1984).

¹⁹ G. Montambaux, M. Héritier, and P. Lederer, Phys. Rev. Lett. **55**, 2078 (1985).

²⁰ J. F. Kwak, J. E. P.M. Chaikin et al., Phys. Rev. Lett. **56**, 972 (1986).

²¹ A. G. Lebed, JETP Lett. **78**, 138 (2003).

²² W. Dieterich and P. Fulde, Z. Phys. **265**, 239 (1973).

²³ P. M. Chaikin, J. Phys. I France **6**, 1875 (1996).

²⁴ D. Zanchi, A. Bjeliš, and G. Montambaux, Phys. Rev. B **53**, 1240 (1996).

²⁵ M. Fujita, K. Machida and H. Nakanishi, J. Phys. Soc Jpn., **54**, 3820 (1985).

²⁶ M.V. Kartsovnik and V.N. Laukin, J. Phys. I France **6**, 1753 (1996).

²⁷ N. Biskup, J.A.A.J. Perenboom, J.S. Qualls, and J.S. Brooks, Solid State Commun. **107**, 503 (1998).

²⁸ P. Christ, W. Biberacher, M. V. Kartsovnik, E. Steep, E. Balthes, H. Weiss, and H. Müller, JETP Lett. **71**, 303 (2000) [Pisma Zh. Eksp. Teor. Fiz. **71**, 437 (2000)].

²⁹ J. S. Qualls, L. Balicas, J. S. Brooks et al., Phys. Rev. B **62**, 10008 (2000).

³⁰ D. Andres, M. V. Kartsovnik, W. Biberacher et al., Phys. Rev. B **64**, 161104(R) (2001).

³¹ N. Harrison, C. H. Mielke, A. D. Christianson, J.S. Brooks, and M. Tokumoto, Phys. Rev. Lett. **86**, 1586 (2001).

³² D. Andres, M. V. Kartsovnik, P. D. Grigoriev, W. Biberacher, and H. Müller, Phys. Rev. B **68**, 201101(R) (2003).

³³ K. Maki, B. Döra, M. V. Kartsovnik et al., Phys. Rev. Lett. **90**, 256402 (2003).

³⁴ N. Harrison, J. Singleton, A. Bangura et al., Phys. Rev. B **69**, 165103 (2004).

³⁵ D. Graf, J. S. Brooks, E. S. Choi et al., Phys. Rev. B **69**, 125113 (2004).

³⁶ D. Graf, E. S. Choi, J. S. Brooks et al., Phys. Rev. Lett. **93**, 076406 (2004).

³⁷ E. B. Lopes, M. J. Matos, R. T. Henriques, M. Almeida, and J. Dumas Phys. Rev. B **52**, R2237 (1995).

³⁸ R. McKenzie, cond-mat/9706235 (1998)

³⁹ A. Bjeliš, D. Zanchi, and G. Montambaux, "Pauli and orbital effects of magnetic field on charge density waves", cond-mat/9909303.

⁴⁰ Y. Hasegawa and H. Fukuyama, J. Phys. Soc. Japan **55**, 3978 (1986).

⁴¹ O. V. Dimitrova and M. V. Feigel'man, JETP Lett. **78**, 637 (2003)

⁴² H. Burkhardt and D. Rainer, Ann. Physik **3**, 181 (1994).